

Ultraviolet Photolysis of CH₂I₂ in Methanol: O–H Insertion and HI Elimination Reactions To Form a Dimethoxymethane Product

Xiangguo Guan, Xufeng Lin, Wai Ming Kwok, Yong Du, Yun-Liang Li, Cunyuan Zhao, Dongqi Wang, and David Lee Phillips*

Department of Chemistry, University of Hong Kong, Pokfulam Road, Hong Kong, PRC

Received: September 1, 2004; In Final Form: November 4, 2004

Ultraviolet photolysis of low concentrations of CH₂I₂ in methanol solution found that CH₂I₂ is converted into dimethoxymethane and some H⁺ and I⁻ products. Picosecond time-resolved resonance Raman (ps-TR³) experiments observed that the isodiodomethane (CH₂I–I) photoproduct decayed faster as the concentration of methanol increases, suggesting that isodiodomethane is reacting with methanol. Ab initio calculations indicate isodiodomethane is able to react with methanol via an O–H insertion/HI elimination to form an iodoether (ICH₂–O–CH₃) and HI products. The iodoether can then further react via another O–H insertion/HI elimination reaction to form the dimethoxymethane (CH₃–O–CH₂–O–CH₃) observed in the photochemistry experiments. A reaction mechanism consistent with these experimental and theoretical observations is proposed.

Introduction

Polyhalomethanes such as CH₂I₂ have been widely used as reagents for addition (such as Kharasch addition) and cyclopropanation of olefins and diiodomethylation of carbonyl compounds.^{1–29} The ultraviolet photolysis of CH₂I₂ in the presence of olefins^{9,17,19,20} leads to formation of cyclopropanated products with a high stereospecificity and a lack of C–H insertion that indicates the carbenoid species is not a free carbene. Ultraviolet photolysis of some other polyhalomethanes such as CHFBr₂, CHClBr₂, CHBr₃, and CHI₃ in the presence of olefins was also found to produce some halocyclopropanated products.^{11,12} Polyhalomethanes can also be activated by metal atoms to form Simmons-Smith type reagents^{1–8,10,14,15,21–29} to carry out a wide range of cyclopropanation reactions. We have recently used a variety of experimental and theoretical methods to elucidate the mechanism of cyclopropanation of olefins that occurs via ultraviolet photolysis of CH₂I₂ in the presence of olefins and have shown that isodiodomethane (CH₂I–I) is the main carbenoid responsible for this type of cyclopropanation reaction.^{30–35} Similar studies also showed that several other isopolyhalomethanes act as effective carbenoid species for cyclopropanation reactions with olefins.^{31,35–38} Comparison of the structures and properties of the isodiodomethane (CH₂I–I) species with the ICH₂ZnI Simmons-Smith carbenoid species showed that their different structures and mode of activation of the methylene carbon could account for their different chemical reactivity toward olefins.^{33–35}

Carbenes and carbenoids such as singlet methylene and dichlorocarbene (:CCl₂) can react with O–H bonds of water to form CH₃OH and CHCl₂OH products, respectively, and can also react with O–H bonds in alcohols.^{39–48} This and the recent direct observation of the isobromoform O–H insertion reaction with water to make a CHBr₂OH reaction product^{49,50} indicate isopolyhalomethanes can also readily undergo O–H insertion reactions with O–H bonds such as other highly reactive carbenoid species. This prompted us to begin to explore the

chemical reactivity of isopolyhalomethanes toward the O–H bonds of alcohols. Here we report a study on the ultraviolet photolysis of CH₂I₂ in methanol solution and find that CH₂I₂ is converted into dimethoxymethane (CH₃–O–CH₂–O–CH₃) and some H⁺ and I⁻ products. Picosecond time-resolved resonance Raman (ps-TR³) spectroscopy experiments done in varying concentrations of methanol found that isodiodomethane (CH₂I–I) photoproduct was formed within several picoseconds after photolysis and decayed faster as the concentration of methanol increases. This suggests that the isodiodomethane intermediate is reacting with methanol. Ab initio calculations indicate that isodiodomethane can react with methanol to form an iodoether (ICH₂–O–CH₃) and HI products. The iodoether can then undergo further reaction with methanol to form the dimethoxymethane observed experimentally in the photochemistry experiments. We propose a reaction mechanism consistent with these experimental and theoretical observations and briefly discuss implications for the chemical reactivity of isopolyhalomethanes toward O–H bonds in alcohols.

Experimental and Computational Details

Photochemistry Experiments. Sample solutions were prepared using commercially available CH₂I₂ (99%), ¹³CH₂I₂, and spectroscopic grade acetonitrile and methanol solvents. Samples of about 1 × 10⁻⁵ M CH₂I₂ in acetonitrile, acetonitrile/methanol, and methanol solvents were contained in a 10-cm path length glass cell with quartz windows. The sample solution was excited by an approximately 3-mJ 266-nm unfocused laser beam from the fourth harmonic of a Nd:YAG laser in the laser photolysis experiments. The absorption spectra for the photolyzed samples were obtained using a 1-cm UV grade cell and a Perkin-Elmer Lambda 19 UV/vis spectrometer. The pH of the photolyzed samples was monitored by a THERRMO Orion 420A pH meter and a 8102BN combination pH electrode. ¹³C and ¹H NMR spectra were obtained from a Bruker Advance 400 DPX spectrometer and ϕ = 5 mm sample tubes at room temperature. The ¹³CH₂I₂ concentration was 1 × 10⁻³ M in methanol and acetonitrile/methanol solvents.

* Corresponding author. E-mail: phillips@hkuc.hku.hk.

Picosecond Time-Resolved Resonance Raman (ps-TR³)

Experiments. The ps-TR³ experiments utilized a newly developed ultrafast laser system in our laboratory that has been described elsewhere,^{49,50} and only a short description will be given here. The pump and probe wavelengths in these experiments were 267 and 400 nm with ~ 15 and $8 \mu\text{J/pulse}$ energy, respectively, and about 1-ps pulse lengths and $\sim 15 \text{ cm}^{-1}$ line-widths. The time-resolution of the system was determined to be about 2 ps, and the time delay between the pump and probe pulses was varied using an optical delay line. The laser beams were lightly focused (about 250 and 150 μm for the pump and probe beams) onto a liquid stream of a re-circulated sample solution with a CH_2I_2 concentration of $\sim 30 \text{ mM}$. The Raman light was acquired using a backscattering geometry and detected by a liquid-nitrogen-cooled CCD detector. The ps-TR³ spectra were found from subtraction of the appropriately scaled probe-before-pump spectrum from the corresponding pump-probe spectrum. The known Raman bands of the solvents were used to calibrate the spectra with an estimated $\pm 5 \text{ cm}^{-1}$ accuracy.

Ab Initio Calculations. The MP2 method was utilized to investigate the $\text{CH}_2\text{I}-\text{I} + n\text{CH}_3\text{OH}$ and $\text{ICH}_2-\text{O}-\text{CH}_3 + n\text{CH}_3\text{OH}$ reactions where $n = 1, 2, 3$. Both the geometry optimization and frequency calculations were done using the 6-31G* basis set for all the C, H, and O atoms and the lan12dz with an additional d polarization of 0.266⁵¹ used for I atoms. All of the computations employed the GAUSSIAN 98 programs.⁵² Intrinsic reaction coordinate (IRC) calculations were performed to confirm the transition states connected the relevant reactants and products.⁵³ The Cartesian coordinates, total energies, and vibrational zero-point energies for the calculated structures are given in the Supporting Information.

Results and Discussion

Photochemistry Experiments. Figure 1(A) shows ultraviolet/visible absorption spectra obtained after 266-nm ultraviolet photolysis of $1 \times 10^{-5} \text{ M}$ CH_2I_2 in methanol solvent. Examination of Figure 1(A) shows that the absorption bands due to CH_2I_2 in the 280–320-nm region decrease in intensity, while those due to the I^- ion in the 220-nm region increase in intensity as the time for photolysis increases. The clear isosbestic point near 253 nm indicates that the I^- is directly produced from the CH_2I_2 parent molecule. The measured molar absorption extinction coefficients for CH_2I_2 and I^- in methanol were used to find the changes in the concentrations of these species as a function of photolysis time, and Figure 1(B) displays a plot of $\Delta[\text{I}^-]$ versus $-\Delta[\text{CH}_2\text{I}_2]$ derived from the spectra of Figure 1(A). The increase in $[\text{I}^-]$ versus the decrease in $[\text{CH}_2\text{I}_2]$ during the photochemistry experiments in Figure 1 shows that there is a linear relationship with a slope of about 2 (1.9 ± 0.2 in Figure 1(B)). This indicates that ultraviolet photolysis of CH_2I_2 at low concentrations in methanol solvent releases two I^- products. The pH was also measured during the photochemistry experiments whose results are shown in Figure 1, and the pH was found to decrease noticeably during the experiment. This indicates that some $[\text{H}^+]$ is also produced during the photochemistry experiments.

To learn more about what product is formed from the carbon atom of the CH_2I_2 product molecule after 266-nm photolysis in methanol, we used a ^{13}C -labeled sample of CH_2I_2 . The 266-nm photolysis experiments were repeated, and ^1H NMR and ^{13}C NMR spectra were acquired before, during, and after photolysis of $^{13}\text{CH}_2\text{I}_2$ in CD_3OD , as shown in Figures 2(A)–2(C). Examination of Figure 2(A) shows that, before photolysis, there

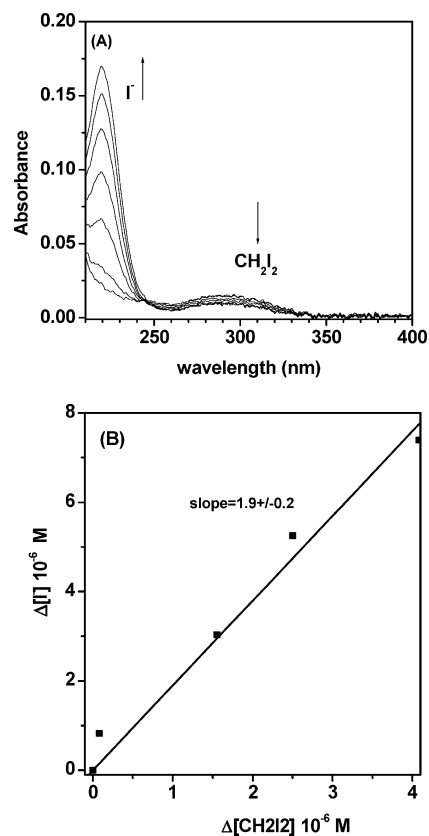
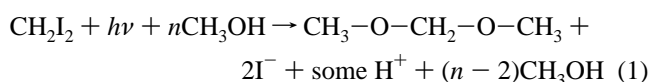


Figure 1. (A) Absorption spectra obtained after varying times of photolysis of a $1 \times 10^{-5} \text{ M}$ CH_2I_2 sample in CH_3OH ; (B) plots of $[\text{I}^-]$ versus $[\text{CH}_2\text{I}_2]$ determined from the spectra of part (A).

is only the parent $^{13}\text{CH}_2\text{I}_2$ band around 3.9 ppm in the ^1H NMR spectrum and -63.9 ppm in the ^{13}C NMR spectrum. During photolysis, the parent $^{13}\text{CH}_2\text{I}_2$ band decreases in intensity and a new photoproduct band appears at about 4.7 ppm in the ^1H NMR spectrum and at 97 ppm in the ^{13}C NMR spectrum. After almost complete photolysis (that is, where the UV–vis absorption spectrum shows the parent $^{13}\text{CH}_2\text{I}_2$ bands have almost disappeared and converted into the I^- band), the parent $^{13}\text{CH}_2\text{I}_2$ band has almost disappeared and the photoproduct bands becomes larger at 4.7 ppm in the ^1H NMR spectrum and at 97 ppm in the ^{13}C NMR spectrum. The characteristic 4.7 ppm band in the ^1H NMR spectrum and 97 ppm in the ^{13}C NMR spectrum of the photoproduct formed after ultraviolet photolysis of $^{13}\text{CH}_2\text{I}_2$ in CD_3OD matches that for dimethoxymethane ($\text{CH}_3-\text{O}-\text{CH}_2-\text{O}-\text{CH}_3$) in the literature. This assignment was confirmed by comparison to an authentic commercial sample of dimethoxymethane, whose ^1H NMR and ^{13}C NMR spectra are shown in Figure 2(D) for comparison purposes.

The preceding experimental photochemistry results indicate that ultraviolet photolysis of CH_2I_2 at low concentrations (such as $1 \times 10^{-5} \text{ M}$) in methanol leads to the following overall reaction:



The experimental results shown in Figures 1 and 2 suggest that this reaction can convert almost all the parent CH_2I_2 compound under low concentration conditions into $\text{CH}_3-\text{O}-\text{CH}_2-\text{O}-\text{CH}_3$ and 2I^- products (with some accompanying H^+ formation). What species produced by ultraviolet photolysis of CH_2I_2 in methanol solutions can lead to efficient reactions to make CH_3-

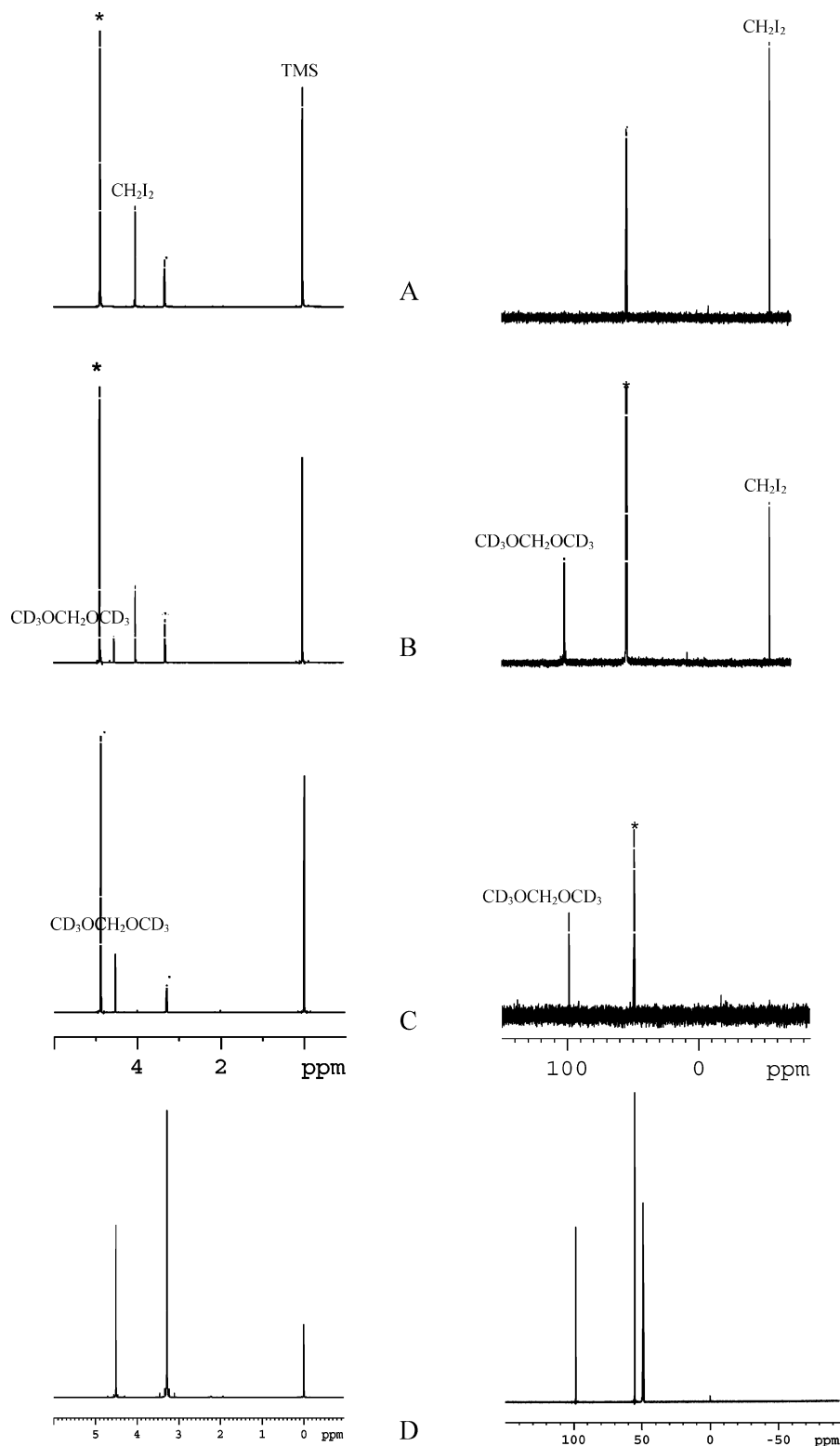


Figure 2. ^1H NMR and ^{13}C NMR spectra obtained (A) before, (B) during, and (C) after 266-nm photolysis of $^{13}\text{CH}_2\text{I}_2$ in CD_3OD . See text for details of the spectra. ^1H NMR and ^{13}C NMR spectra are also shown in (D) for an authentic commercial sample of $\text{CH}_3\text{-O-CH}_2\text{-O-CH}_3$. (* indicate solvent peaks).

$\text{O-CH}_2\text{-O-CH}_3$ and 2I^- products accompanied by some H^+ formation? To help answer this question, time-resolved experiments and ab initio calculations were done to investigate the chemical intermediates and their reactions with methanol, and these results are detailed in the next two sections.

Picosecond Time-Resolved Resonance Raman (Ps-TR³) Experiments. Figure 3 presents ps-TR³ spectra acquired for the photoproducts produced after 267-nm photolysis of CH_2I_2

in acetonitrile, 90% acetonitrile/10% methanol, and methanol solvents using a 400-nm probe wavelength. The spectra shown in Figure 3 are in excellent agreement with those reported for the isodiiodomethane species ($\text{CH}_2\text{-I}$) in mixed acetonitrile/water solvents and water/methanol solvents.^{54,55} The Raman bands observed in Figure 3 are readily assigned to the $\text{CH}_2\text{-I}$ intermediate, and the reader is referred to refs 32, 54, 56, and 57 for details of the vibrational assignments. Inspection of Figure

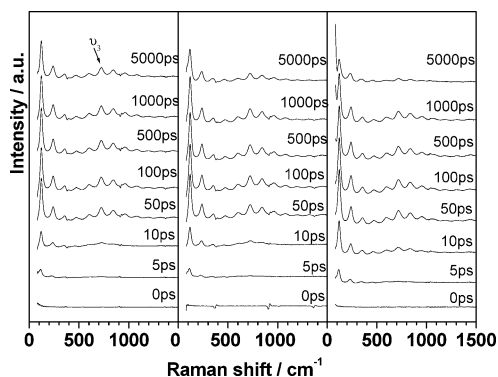


Figure 3. Ps-TR³ spectra obtained for the photoproducts produced after 267-nm photolysis of CH₂I₂ in acetonitrile, 90% acetonitrile/10% methanol, and methanol solvents using a 400-nm probe wavelength. The time delay between the pump and probe beams is shown in picoseconds to the right of each spectrum.

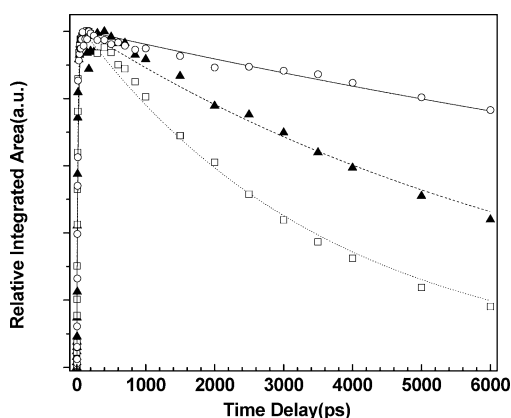


Figure 4. Plots of the relative integrated area of the ν_3 Raman band of CH₂I-I at different delay times (from 0 to 6000 ps) obtained in CH₃OH (open squares), 90% CH₃CN/10% CH₃OH (solid triangles), and CH₃CN (open circles) solvents, respectively. The dotted line (CH₃OH), dashed line (90% CH₃CN/10% CH₃OH), and solid line (CH₃CN) represent least-squares fits to the data.

3 shows that the CH₂I-I photoproduct Raman bands appear within several picoseconds and then decay faster as the concentration of methanol increases.

The resonance Raman band near 715 cm⁻¹ assigned to the fundamental nominal C-I stretch mode (ν_3) was integrated at different time delays in order to extract the kinetics of the growth and decay of the CH₂I-I species. Figure 4 display plots of the relative integrated area of the ν_3 Raman band from 0 to 6000 ps in the acetonitrile (open circles), 90% acetonitrile/10% methanol (solid triangles), and methanol (open squares) solvents. The relative integrated areas of the ν_3 Raman bands were fit to a simple function (the solid, dashed, and dotted lines in Figure 4 represent these fits):

$$I(t) = Ae^{-t/t_1} - Be^{-t/t_2} \quad (2)$$

where $I(t)$ is the relative integrated area of the ν_3 Raman band, t is the time, t_1 is the decay time-constant of the ν_3 Raman band, t_2 is the growth time-constant of the ν_3 Raman band, and A and B are constants. The fits to the data in Figure 3 determined that the CH₂I-I photoproduct had similar time-constants (t_2) of 20, 18, and 15 ps for its growth. However, the decay of CH₂I-I varied greatly as a function of the methanol concentration and (t_1) of >20 000, 7641, and 3654 ps for its decay in the acetonitrile, 90% acetonitrile/10% methanol, and methanol

solvents, respectively. The CH₂I-I Raman bands decay with the lifetime decreasing significantly as the methanol concentration increases, suggesting CH₂I-I may be reacting with the methanol molecules.

A recent study found the CH₂I-I species decays with a rate constant of $4.3 \times 10^6 \text{ s}^{-1}$ in pure acetonitrile solvent where this decay was attributed to CH₂I-I decaying into a CH₂I radical and I atom accompanied by some decay into an I⁻ product.⁵⁸ We note that the decay of CH₂I-I in pure methanol, $k = 1.3 \times 10^8 \text{ s}^{-1}$ from ref 54 and from our present study, is more than 2 orders of magnitude faster than in pure acetonitrile even though the dielectric constants of these solvents are similar (33.1 for methanol and 38.8 for acetonitrile at 20 °C). It is interesting that the decay of CH₂I-I in methanol is similar to that for 25% to 50% water in acetonitrile solvent that had measured decay times of 4640 ps to 1860 ps and corresponding rate constants of $k = 2.2 \times 10^8 \text{ s}^{-1}$ and $5.4 \times 10^8 \text{ s}^{-1}$, respectively.^{54,55} This similarity is consistent with the CH₂I-I species undergoing O-H insertion reactions with the O-H bond of methanol and the O-H bonds of water, while there is no possible O-H insertion reaction for the acetonitrile solvent. These O-H insertion reactions would help explain why the decomposition of CH₂I-I is much slower in acetonitrile solvent than in pure methanol or mixed water/acetonitrile solvents.^{54,55,58} The recent direct observation of the isobromofrom O-H insertion reaction with water to produce a CHBr₂OH reaction product^{49,50} suggests that CH₂I-I would likely also undergo a similar O-H insertion reaction with water and methanol, insofar as CH₂I-I has a chemical reactivity similar to isobromofrom and other carbenoid species. Recent ab initio calculations also indicate that CH₂I-I undergoes O-H insertion/HI elimination reactions with water to produce iodomethanol (CH₂IOH) and HI products.⁵⁵ In the next section, we have done similar ab initio calculations to explore the chemical reactivity of CH₂I-I toward the O-H bonds of methanol.

Ab Initio Calculations. Figures 5 and 6 present the optimized geometry and Figure 7 presents schematic diagrams of the relative energy profiles (in kcal/mol) obtained from the MP2 calculations for the reactant complexes, transition states, and product complexes of the following reactions: CH₂I-I + n CH₃OH → CH₃-O-CH₂I + HI + ($n - 1$)CH₃OH, and ICH₂-O-CH₃ + n CH₃OH → CH₃-O-CH₂-O-CH₃ + HI + ($n - 1$)CH₃OH where $n = 1, 2, 3$.

Inspection of Figure 7 reveals the CH₂I-I + CH₃OH → CH₃-O-CH₂I + HI reaction occurs with an estimated barrier of 9.9 kcal/mol from its reactant complex to its transition state. As more methanol molecules are explicitly considered in the reaction, the barrier reaction decreases to 7.7 kcal/mol for $n = 2$ and then to 6.1 kcal/mol for $n = 3$ methanol molecules. This suggests that additional methanol molecules can catalyze or accelerate the O-H insertion/HI elimination reaction. As the starting materials for the first reaction (SM) proceed to the reactant complex, the C-I-I angle of isodiodomethane goes from 118.0 degrees in SM to 114.5 degrees in RC11, 116.3 degrees in RC12, and 115.7 degrees in RC13. In addition, the I-I bond length gets a little weaker, going from 3.030 Å in SM to 3.043 Å in RC11, 3.052 Å in RC12, and 3.057 Å in RC13. These changes are consistent with complex formation, moderate stabilization of the reactant complex, and moderate solvation of the terminal I atom.

The optimized geometry structures in Figure 5 show that, as the reactant complexes go to their transition states, the I-I bonds lengths, the C-O bond distance decreases, the H-I distance decreases, and the O-H bond of the methanol closest to the

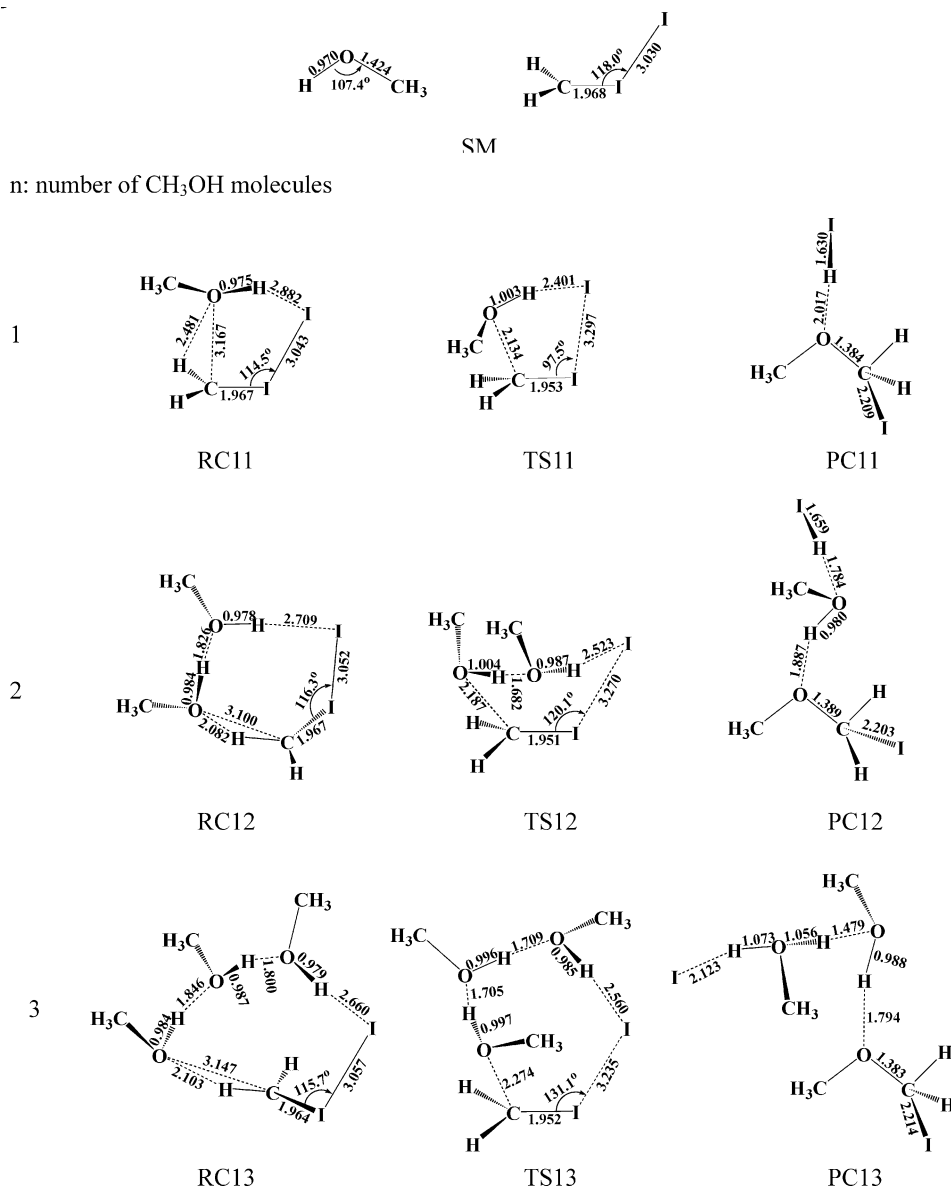


Figure 5. Schematic diagrams are shown for the reactant complexes (RC11–RC13), transition states (TS11–TS13), and product complexes (PC11–PC13) for the reactions of $\text{CH}_2\text{I}-\text{I} + n\text{CH}_3\text{OH} \rightarrow \text{CH}_3-\text{O}-\text{CH}_2\text{I} + \text{HI} + (n-1)\text{CH}_3\text{OH}$ where $n = 1, 2, 3$. The optimized species for these species were obtained from MP2 calculations using the 6-31G* basis set for all the C, H, and O atoms and the lan12dz basis set with an additional *d* polarization of 0.266 for the I atoms. Selected bond length (in Å) and bond angle (in degrees) parameters are shown.

terminal I atom becomes longer. For example, the I–I bonds go from a bond length of 3.043 Å in RC11 to 3.297 Å in TS11, from 3.052 Å in RC12 to 3.270 Å in TS11, and from 3.057 Å in RC13 to 3.235 Å in TS13. The C–O bond distance decreases from 3.167 Å in RC11 to 2.134 Å in TS11, from 3.100 Å in RC12 to 2.187 Å in TS12, and from 3.147 Å in RC13 to 2.274 Å in TS13. The H–I distance decreases from 2.882 Å in RC11 to 2.401 Å in TS11, 2.709 Å in RC12 to 2.523 Å in TS12 and 2.660 Å in RC13 to 2.560 Å in TS13. The O–H bond of the methanol closest to the terminal I atom goes from 0.975 Å in RC11 to 1.003 Å in TS11, from 0.978 Å in RC12 to 0.987 Å in TS12, and from 0.979 Å in RC13 to 0.985 Å in TS13. These structural changes indicate that there is partial bond formation of the C–O and H–I bonds in the TSs accompanied by partial bond cleavage and/or weakening of the I–I and O–H bonds. These changes are consistent with an O–H insertion/HI elimination reaction taking place to produce $\text{CH}_3-\text{O}-\text{CH}_2\text{I} + \text{HI}$. This was confirmed by IRC calculations, and a vibrational frequency of 395.7i cm^{-1} was found for TS11. These

results are very similar to those previously found for the analogous O–H insertion/HI elimination reaction of isodiiodomethane with water ($\text{CH}_2\text{I}-\text{I} + n\text{H}_2\text{O} \rightarrow \text{HO}-\text{CH}_2\text{I} + (n-1)\text{HI}$) from its reactant complexes to their respective transition states.⁵⁵ As the number of methanol molecules in the reaction increases, there are generally smaller structural changes occurring from the RCs to their respective TSs, suggesting that less energy is needed to go from the RC to the TS as more methanol molecules are present. This is consistent with the barrier-to-reaction decrease as more methanol molecules are incorporated into the reaction system and very similar to the behavior previously observed for the water-catalyzed O–H insertion/HI elimination reaction of isodiiodomethane with water ($\text{CH}_2\text{I}-\text{I} + n\text{H}_2\text{O} \rightarrow \text{HO}-\text{CH}_2\text{I} + (n-1)\text{HI}$).⁵⁵ The low barrier to reaction near 6.1 kcal/mol for $n = 3$ methanol molecules is consistent with the fast reaction of $\text{CH}_2\text{I}-\text{I}$ with methanol observed in the ps-TR³ experiments and suggests that the O–H insertion/HI elimination reaction of methanol with $\text{CH}_2\text{I}-\text{I}$ can account for this.

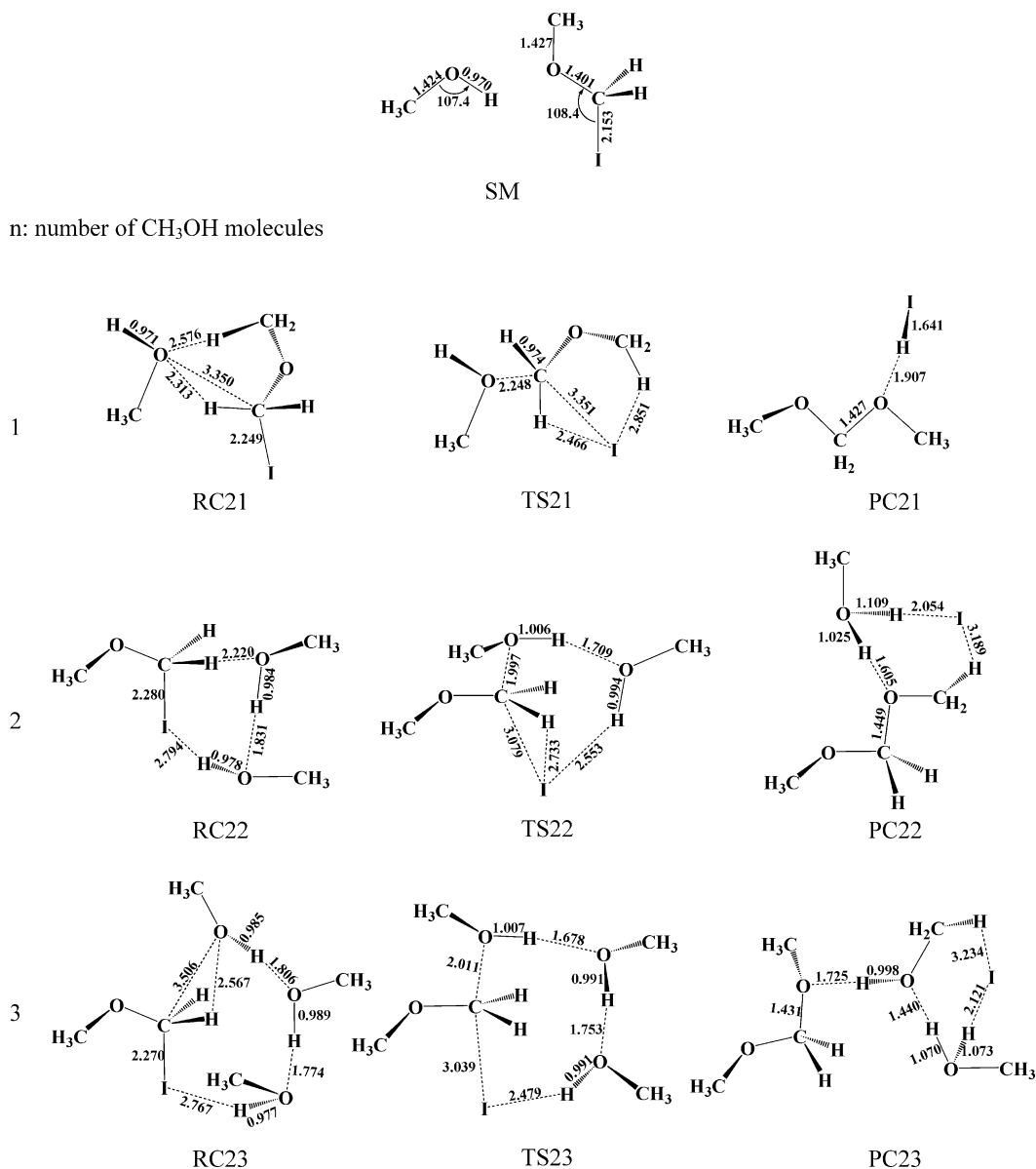


Figure 6. Schematic diagrams are shown for the reactant complexes (RC21–RC23), transition states (TS21–TS23), and product complexes (PC21–PC23) for the reactions of $\text{ICH}_2\text{--O--CH}_3 + n\text{CH}_3\text{OH} \rightarrow \text{CH}_3\text{--O--CH}_2\text{--O--CH}_3 + \text{HI} + (n-1)\text{CH}_3\text{OH}$ where $n = 1, 2, 3$. The optimized species for these species were obtained from MP2 calculations using the basis sets described in Figure 5. Selected bond length (in Å) and bond angle (in degrees) parameters are shown.

The iodoether ($\text{CH}_3\text{--O--CH}_2\text{I}$) product can then undergo further reaction with a methanol via a similar reaction. Examination of Figure 7 shows that the $\text{CH}_3\text{--O--CH}_2\text{I} + \text{CH}_3\text{OH} \rightarrow \text{CH}_3\text{--O--CH}_2\text{--O--CH}_3 + \text{HI}$ reaction occurs with an estimated barrier of 35.2 kcal/mol from its reactant complex to its transition state. As more methanol molecules are considered in the reaction, the barrier to reaction decreases to 24.3 kcal/mol for $n = 2$ and then to 15.8 kcal/mol for $n = 3$ methanol molecules and may decrease further as more methanol molecules are added. This suggests that additional methanol molecules can catalyze or accelerate the O–H insertion/HI elimination reaction. The optimized geometry structures in Figure 6 reveal that as the reactant complexes go to their transition states, the C–I bonds lengthens, the C–O bond distance decreases, and the H–I distance decreases. These structural changes indicate that there is partial bond formation of the C–O and H–I bonds in the TSs, accompanied by partial bond cleavage and/or weakening of the C–I bonds. These changes are consistent with an O–H insertion/HI elimination reaction taking place to produce $\text{CH}_3\text{--}$

$\text{O--CH}_2\text{--O--CH}_3 + \text{HI}$ products. These results are very similar to those previously found for the preceding O–H insertion/HI elimination reaction of isodiiodomethane with methanol ($\text{CH}_2\text{I--I} + n\text{CH}_3\text{OH} \rightarrow \text{CH}_3\text{--O--CH}_2\text{I} + \text{HI} + (n-1)\text{CH}_3\text{OH}$) and the analogous O–H insertion/HI elimination reaction of isodiiodomethane with water ($\text{CH}_2\text{I--I} + n\text{H}_2\text{O} \rightarrow \text{HO--CH}_2\text{I} + (n-1)\text{HI}$) from its reactant complexes to their respective transition states.⁵⁵ As the number of methanol molecules in the reaction increases, there are generally smaller structural changes occurring from the RCs to their respective TSs, suggesting that less energy is needed to go from the RC to the TS as more methanol molecules are present and is also consistent with the barrier-to-reaction decrease as more methanol molecules are incorporated into the reaction system.

Proposed Reaction Mechanism. The ab initio calculation results in conjunction with the time-resolved spectroscopy experimental results suggest a probable reaction mechanism for formation of the $\text{CH}_3\text{--O--CH}_2\text{--O--CH}_3$ and 2I^- products (plus

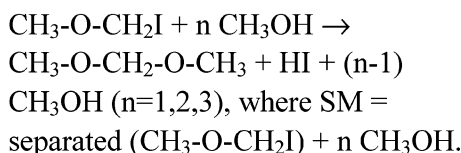
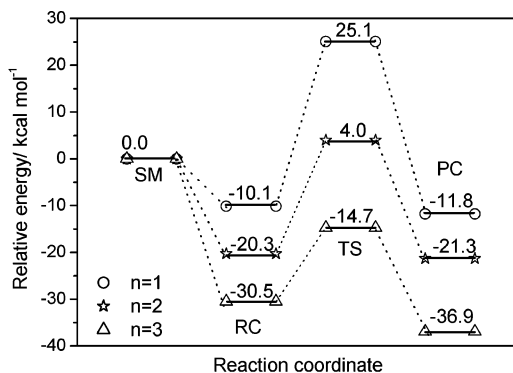
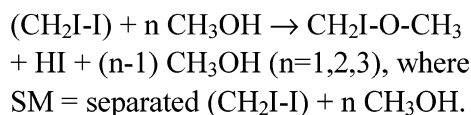
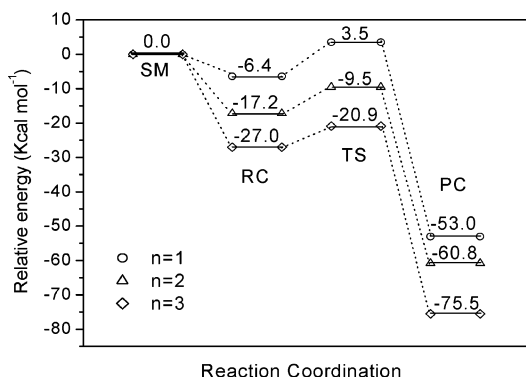
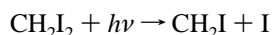


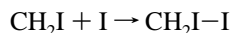
Figure 7. Schematic diagrams of the energy profile (in kcal/mol) obtained from the MP2 calculations for the reactions of $\text{CH}_2\text{I}-\text{I} + n\text{CH}_3\text{OH} \rightarrow \text{CH}_3-\text{O}-\text{CH}_2\text{I} + \text{HI} + (n-1)\text{CH}_3\text{OH}$ and $\text{ICH}_2-\text{O}-\text{CH}_3 + n\text{CH}_3\text{OH} \rightarrow \text{CH}_3-\text{O}-\text{CH}_2-\text{O}-\text{CH}_3 + \text{HI} + (n-1)\text{CH}_3\text{OH}$ where $n = 1, 2, 3$.

some accompanying H^+) observed in the photochemistry experiments. This reaction mechanism is shown below.

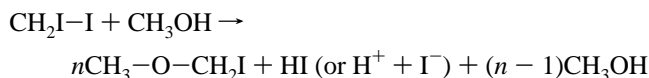
Step 1. Photodissociation of CH_2I_2 :



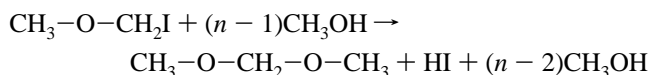
Step 2. Solvent-induced geminate recombination to produce isodiodomethane:



Step 3. O-H insertion/HI elimination reaction of $\text{CH}_2\text{I}-\text{I}$ with methanol:

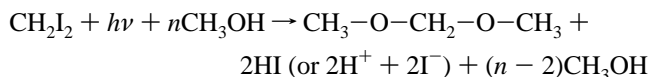


Step 4. O-H insertion/HI elimination reaction of iodoether with methanol:



Add steps 1–4 to obtain the overall reaction.

Overall Reaction:



The proposed reaction mechanism shown above can help explain how the ultraviolet photolysis of low concentrations of CH_2I_2 in methanol leads to formation of the $\text{CH}_3-\text{O}-\text{CH}_2-\text{O}-\text{CH}_3$ and 2I^- products (plus some accompanying H^+) observed in the photochemistry experiments described in this work. It is well-known that ultraviolet excitation of CH_2I_2 in both gas and solutions phases leads to direct C–I bond cleavage to form a CH_2I radical and I atom, and this indicates that step 1 is the primary photochemical initiation of the reaction.^{59–65} Time-resolved experiments have established that solvent-induced geminate recombination of these CH_2I and I fragments can form appreciable amounts of the isodiodomethane ($\text{CH}_2\text{I}-\text{I}$) intermediate in a number of solvents including methanol (see Figure 3), and this indicates that step 2 of the proposed reaction mechanism occurs to a significant degree. In addition, a very

nice theoretical study by another group used molecular dynamics simulations to elucidate how the initially formed CH_2I radical and I atom fragments recombine in acetonitrile solution to produce the $\text{CH}_2\text{I}-\text{I}$ intermediate.⁶⁶ This provides additional support for step 2 of the proposed reaction mechanism. The substantially faster decay of the $\text{CH}_2\text{I}-\text{I}$ species in the presence of methanol (see Figures 3 and 4) suggests that $\text{CH}_2\text{I}-\text{I}$ is reacting with methanol. This, in conjunction with the ab initio calculation results, indicates that $\text{CH}_2\text{I}-\text{I}$ reacts with CH_3OH via an O–H insertion/HI elimination reaction to produce an iodoether ($\text{CH}_3\text{OCH}_2\text{I}$) product and HI product, consistent with step 3 of the proposed reaction mechanism.

We note that iodoether ($\text{CH}_3\text{OCH}_2\text{I}$) is a commercially available compound. We dissolved an authentic sample of iodoether in methanol (CD_3OD) and acetonitrile (CD_3CN) solvents and acquired ^1H NMR spectra as shown in Figure 8. The parent CH_2IOCH_3 bands appear at about 3.3 and 5.8 ppm in the ^1H NMR spectrum obtained in acetonitrile (CD_3CN) solvent (Figure 8(B)). When iodoether ($\text{CH}_3\text{OCH}_2\text{I}$) is dissolved in methanol (CD_3OD), it is converted into $\text{CD}_3-\text{O}-\text{CH}_2-\text{O}-\text{CH}_3$ product with its characteristic 4.7 ppm band (Figure 8(A)). We then obtained ^1H NMR spectra for 10 μL of iodoether ($\text{CH}_3\text{OCH}_2\text{I}$) dissolved in CD_3CN with amounts of CD_3OD added from 2 μL to 10 μL as shown in Figure 9. As the amount of CD_3OD added increases, more of the parent iodoether ($\text{CH}_3\text{OCH}_2\text{I}$) is converted into $\text{CD}_3-\text{O}-\text{CH}_2-\text{O}-\text{CH}_3$ product with its characteristic 4.7 ppm band. The results in Figures 8 and 9 indicate that iodoether ($\text{CH}_3\text{OCH}_2\text{I}$) may react with methanol to produce the $\text{CD}_3-\text{O}-\text{CH}_2-\text{O}-\text{CH}_3$ dimethoxy-methane product. These experimental results, in conjunction with the ab initio results in Figures 6 and 7 for the O–H insertion/HI elimination reaction of $n\text{CH}_3\text{OH}$ with iodoether, provides support for step 4 of the proposed reaction mechanism. The proposed reaction mechanism is consistent with a range of experimental and theoretical results shown here and in the literature for the photodissociation of CH_2I_2 in room-temperature solutions and provides a reasonable explanation for how the ultraviolet photolysis of CH_2I_2 in methanol leads to formation of $\text{CH}_3-\text{O}-\text{CH}_2-\text{O}-\text{CH}_3$ and 2I^- products (plus some accompanying H^+) observed in the photochemistry experiments.

Brief Discussion of Chemical Reactivity of Isopolyhalomethanes toward O–H Bonds of Alcohols. Our present study indicates that isodiodomethane ($\text{CH}_2\text{I}-\text{I}$) reacts with methanol

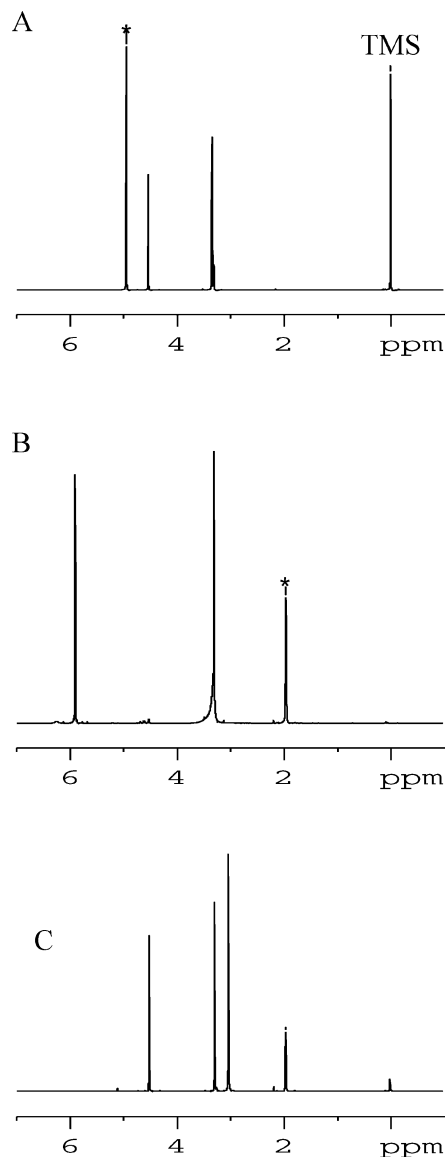


Figure 8. ^1H NMR spectra obtained CH_2IOCH_3 in (A) CD_3OD , (B) CD_3CN , and (C) CD_3CN with a small amount of CD_3OD added. The parent iodoether bands appear at about 3.3 and 5.8 ppm in the ^1H NMR spectra in CD_3CN . In CD_3OD solvent, iodoether is converted into $\text{CD}_3\text{OCH}_2\text{OCH}_3$ product whose characteristic band is at 4.7 ppm (A). With the addition of small amounts of CD_3OD in CD_3CN , iodoether is also converted into $\text{CD}_3\text{OCH}_2\text{OCH}_3$ product whose characteristic band is at 4.7 ppm (C). (* indicate solvent peaks).

via an O–H insertion/HI elimination reaction to produce an iodoether ($\text{CH}_3\text{—O—CH}_2\text{I}$) product and a HI (or H^+ and I^-) product. This is very similar to the reaction of isodiodomethane ($\text{CH}_2\text{I—I}$) with water via an O–H insertion/HI elimination reaction to produce an iodomethanol ($\text{HO—CH}_2\text{I}$) product and a HI (or H^+ and I^-) product.⁵⁵ The bond strength of the O–H bond of methanol ($D_{298}^0 = 104.4 \pm 1$ kcal/mol) is modestly weaker than the O–H bond in water ($D_{298}^0 = 119 \pm 1$ kcal/mol), and this suggests that the O–H bond in methanol may be easier to break and undergo an O–H insertion reaction than an O–H bond in water. This appears consistent with the results of the MP2 calculations that show the $\text{CH}_2\text{I—I} + \text{CH}_3\text{OH} \rightarrow \text{CH}_3\text{—O—CH}_2\text{I} + \text{HI}$ reaction has a barrier height of about 9.9 kcal/mol from its RC11 to its TS11 while the $\text{CH}_2\text{I—I} + \text{H}_2\text{O} \rightarrow \text{HO—CH}_2\text{I} + \text{HI}$ reaction has a barrier height of about 13.6 kcal/mol from its RC to its TS.⁵⁵ This suggests that an isopolyhalomethane carbenoid may more readily undergo an

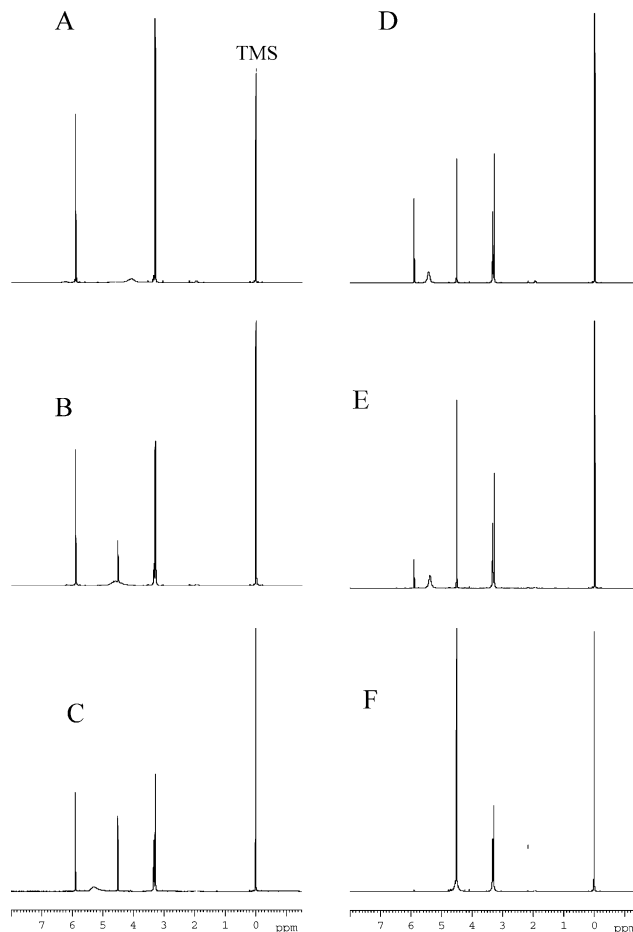


Figure 9. ^1H NMR spectra obtained for 10 μL of iodoether (CH_2IOCH_3) in CD_3CN solvent with varying amounts of CD_3OD added to the solution: 0 μL (A), 2 μL (B), 4 μL (C), 6 μL (D), 8 μL (E), and 10 μL (F). The parent iodoether (CH_2IOCH_3) bands appear at about 3.3 and 5.8 ppm, and the $\text{CD}_3\text{OCH}_2\text{OCH}_3$ product band is at 4.7 ppm in the ^1H NMR spectra. See text for more details.

O–H insertion/HX elimination with an alcohol O–H bond than with a water O–H bond. However, the explicit incorporation of additional water molecules in the reaction system (that is, the $\text{CH}_2\text{I—I} + n\text{H}_2\text{O} \rightarrow \text{HO—CH}_2\text{I} + \text{HI} + (n - 1)\text{H}_2\text{O}$ reaction) found that water substantially catalyzes the reaction through its O–H bonding interactions with the reaction system and the barrier to reaction decreased to only 3.8 kcal/mol for $n = 3$ water molecules. However, the methyl moiety may add significant steric hindrance for forming an effective solvent O–H bonding structure to best catalyze the reaction system, and this effect may account for why the $\text{CH}_2\text{I—I} + \text{CH}_3\text{OH} \rightarrow \text{CH}_3\text{—O—CH}_2\text{I} + \text{HI}$ reaction has a barrier height that decreases more slowly as the number of water molecules increases (for example, to 6.1 kcal/mol for $n = 3$ methanol molecules). This steric effect would be expected to become more noticeable for larger alcohols. Further experimental and theoretical work is needed to address the relative ability of the larger alcohols compared to methanol to catalyze these types of O–H insertion/HX elimination reactions.

Conclusion

A combined experimental and theoretical study was done to examine the ultraviolet photolysis of low concentrations of CH_2I_2 in methanol solution. Photochemistry experiments observed that CH_2I_2 was converted into $\text{CH}_3\text{—O—CH}_2\text{—O—CH}_3$ and some H^+ and I^- products. Picosecond time-resolved

resonance Raman (ps-TR³) spectroscopy experiments observed that the isodiiodomethane (CH₂I-I) photoproduct was produced within several picoseconds after photolysis and then decayed faster as the concentration of methanol increases, suggesting that isodiiodomethane is reacting with methanol. Ab initio MP2 calculations indicate that isodiiodomethane can undergo an O-H insertion/HI elimination reaction with methanol to produce an iodoether (ICH₂-O-CH₃) product accompanied by a HI product. The ab initio calculations also indicate iodoether can then further react with methanol (*n*CH₃OH) via an O-H insertion/HI elimination reaction to form another HI leaving group and the CH₃-O-CH₂-O-CH₃ observed experimentally in the photochemistry experiments. Further experiments showed that an authentic commercially available sample of iodoether readily reacts with methanol to produce a CH₃-O-CH₂-O-CH₃ product, consistent with the predictions of the ab initio calculations and iodoether being an intermediate in the photochemistry experiments. A reaction mechanism consistent with these experimental and theoretical observations was proposed. Likely implications for the chemical reactivity of isopolyhalomethanes toward O-H bonds in alcohols was very briefly discussed.

Acknowledgment. This research has been supported by grants from the Research Grants Council of Hong Kong (HKU/7021/03P and HKU 1/01C) to D.L.P. W.M.K. thanks the University of Hong Kong for the award of a Postdoctoral Fellowship.

Supporting Information Available: Selected output from the MP2 ab initio calculations giving the Cartesian coordinates, total energies, and vibrational zero-point energies for the stationary structures shown in Figures 5 and 6. This material is available free of charge via the Internet at <http://pubs.acs.org>.

References and Notes

- (1) Walling, C.; Huyser, E. S. *Org. React.* **1967**, *13*, 91–149.
- (2) Lüsberg, S.; Godfredsen, W. O.; Vangedal, S. *Tetrahedron* **1960**, *9*, 149–155.
- (3) *The Chemistry of the Cyclopropyl Group*; Rappoport, Z., Ed.; Wiley: Chichester, 1987.
- (4) Lebel, H.; Marcoux, J.-F.; Molinaro, C.; Charette, A. B. *Chem. Rev.* **2003**, *103*, 977–1050.
- (5) Denmark, S. E.; Beutner, G. *Cycloaddition Reactions in Organic Synthesis*; Wiley-VCH: New York, 2002; Chapter 3, pp 85–150.
- (6) Simmons, H. E.; Smith, R. D. *J. Am. Chem. Soc.* **1958**, *80*, 5323–5324.
- (7) Simmons, H. E.; Smith, R. D. *J. Am. Chem. Soc.* **1959**, *81*, 4256–4264.
- (8) Wittig, G.; Schwarzenbach, K. *Angew. Chem.* **1959**, *20*, 652–653.
- (9) Blomstrom, D. C.; Herbig, K.; Simmons, H. E. *J. Org. Chem.* **1965**, *30*, 959–964.
- (10) Furukawa, J.; Kawabata, N.; Nishimura, J. *Tetrahedron Lett.* **1966**, *7*, 3353–3354.
- (11) Marolewski, T.; Yang, N. C. *J. Chem. Soc., Chem. Commun.* **1967**, 1225–1226.
- (12) Yang, N. C.; Marolewski, T. *J. Am. Chem. Soc.* **1968**, *90*, 5644–5646.
- (13) Sawada, S.; Oda, J.; Iouye, Y. *J. Org. Chem.* **1968**, *33*, 2141–2153.
- (14) Furukawa, J.; Kawabata, N.; Nishimura, J. *Tetrahedron* **1968**, *24*, 53–58.
- (15) Poulter, C. D.; Friedrich, E. C.; Winstein, S. *J. Am. Chem. Soc.* **1969**, *91*, 6892–6894.
- (16) Kawabata, N.; Nakagawa, T.; Nakao, T.; Yamashita, S. *J. Org. Chem.* **1977**, *42*, 3031–3035.
- (17) Pienta, N. J.; Kropp, P. J. *J. Am. Chem. Soc.* **1978**, *100*, 655–657.
- (18) Rieke, R. D.; Tzu-Jung, L. P.; Burns, T. P.; Uhm, S. T. *J. Org. Chem.* **1981**, *46*, 4323–4324.
- (19) Kropp, P. J.; Pienta, N. J.; Sawyer, J. A.; Polniaszek, R. P. *Tetrahedron* **1981**, *37*, 3229–3236.
- (20) Kropp, P. J. *Acc. Chem. Res.* **1984**, *17*, 131–137.

- (21) Marouka, K.; Fukutani, Y.; Yamamoto, H. *J. Org. Chem.* **1985**, *50*, 4412–4414.
- (22) Friedrich, E. C.; Domek, J. M.; Pong, R. Y. *J. Org. Chem.* **1985**, *50*, 4640–4642.
- (23) Friedrich, E. C.; Lunetta, S. E.; Lewis, E. J. *J. Org. Chem.* **1989**, *54*, 2388–2390.
- (24) Molander, G. A.; Harring, L. S. *J. Org. Chem.* **1989**, *54*, 3525–3532.
- (25) Durandetti, S.; Sibille, S.; Périchon, J. *J. Org. Chem.* **1991**, *56*, 3255–3258.
- (26) Yang, Z. Q.; Lorenz, J. C.; Shi, Y. *Tetrahedron Lett.* **1998**, *39*, 8621–8624.
- (27) Charette, A. B.; Marcoux, J.-F.; Molinaro, C.; Beauchemin, A.; Brochu, C.; Isabel, É. *J. Am. Chem. Soc. (Commun.)* **2000**, *122*, 4508–4509.
- (28) Charette, A. B.; Francoeur, S.; Martel, J.; Wilb, N. *Angew. Chem., Int. Ed.* **2000**, *39*, 4539–4542.
- (29) For crystal structures of typical Zn-based carbenoids, see (a) Denmark, S. E.; Edwards, J. P.; Wilson, S. R. *J. Am. Chem. Soc.* **1991**, *113*, 723–725. (b) Denmark, S. E.; Edwards, J. P.; Wilson, S. R. *J. Am. Chem. Soc.* **1992**, *114*, 2592–2602. (c) Charette, A. B.; Marcoux, J.-F.; Bélanger-Gariépy, F. *J. Am. Chem. Soc. (Commun.)* **1996**, *118*, 6792–6793.
- (30) Phillips, D. L.; Fang, W.-H.; Zheng, X. *J. Am. Chem. Soc.* **2001**, *123*, 4197–4203.
- (31) Phillips, D. L.; Fang, W.-H. *J. Org. Chem.* **2001**, *66*, 5890–5896.
- (32) Li, Y.-L.; Leung, K. H.; Phillips, D. L. *J. Phys. Chem. A* **2001**, *105*, 10621–10625.
- (33) Fang, W.-H.; Phillips, D. L.; Wang, D.; Li, Y.-L. *J. Org. Chem.* **2002**, *67*, 154–160.
- (34) Li, Y.-L.; Wang, D.; Phillips, D. L. *J. Chem. Phys.* **2002**, *117*, 7931–7941.
- (35) Phillips, D. L.; Fang, W.-H.; Zheng, X.; Li, Y.-L.; Wang, D.; Kwok, W. M. *Curr. Org. Chem.* **2004**, *8*, 739–755.
- (36) Zheng, X.; Fang, W. H.; Phillips, D. L. *J. Chem. Phys.* **2000**, *113*, 10934–10946.
- (37) Zheng, X.; Lee, C. W.; Li, Y. L.; Fang, W. H.; Phillips, D. L. *J. Chem. Phys.* **2001**, *114*, 8347–8356.
- (38) Li, Y.-L.; Chen, D. M.; Wang, D.; Phillips, D. L. *J. Org. Chem.* **2002**, *67*, 4228–4235.
- (39) Harding, L. B.; Schlegel, H. B.; Krishnan, R.; Pople, J. A. *J. Phys. Chem.* **1980**, *84*, 3394–3401.
- (40) Pople, J. A.; Raghavachari, K.; Frisch, M. J.; Binkley, J. B.; Schleyer, P. V. R. *J. Am. Chem. Soc.* **1983**, *105*, 6389–6398.
- (41) Wesdemiotis, C.; Feng, R.; Danis, P. O.; Williams, E. R.; Lafferty, F. W. *J. Am. Chem. Soc.* **1986**, *108*, 5847–5853.
- (42) Yates, B. F.; Bouma, W. J.; Radom, L. *J. Am. Chem. Soc.* **1987**, *109*, 2250–2263.
- (43) Kirmse, W.; Meinert, T.; Moderelli, D. A.; Platz, M. S. *J. Am. Chem. Soc.* **1993**, *115*, 8918–8927.
- (44) Walch, S. P. *J. Chem. Phys.* **1993**, *98*, 3163–3178.
- (45) Gonzalez, C.; Restrepo-Cossio, A.; Márquez, M.; Wiberg, K. B. *J. Am. Chem. Soc.* **1996**, *118*, 5408–5411.
- (46) Moody, C. J.; Whitman, G. H. In *Reactive Intermediates*; Davies, S. G., Ed.; Oxford University Press: New York, 1992.
- (47) Pliego, J. R., Jr.; De Almeida, W. B. *J. Phys. Chem.* **1996**, *100*, 12410–12413.
- (48) Pliego, J. R., Jr.; De Almeida, W. B. *J. Phys. Chem. A* **1999**, *103*, 3904–3909.
- (49) Kwok, W. M.; Zhao, C.; Li, Y. L.; Guan, X.; Phillips, D. L. *J. Chem. Phys.* **2004**, *120*, 3323–3332.
- (50) Kwok, W. M.; Zhao, C.; Li, Y. L.; Guan, X.; Wang, D.; Phillips, D. L. *J. Am. Chem. Soc.* **2004**, *126*, 3119–3131.
- (51) Huzinaga, S.; Anzelm, J.; Klobukowski, M.; Radzio-Andzelm, E.; Sakai, Y.; Tatewaki, H. In *Gaussian Basis Sets for Molecular Calculations*; Elsevier: Amsterdam, 1984.
- (52) Frisch, M. J.; Trucks, G. W.; Schlegel, H. B.; Scuseria, G. E.; Robb, M. A.; Cheeseman, J. R.; Zakrzewski, V. G.; Montgomery, J. A., Jr.; Stratmann, R. E.; Burant, J. C.; Dapprich, S.; Millam, J. M.; Daniels, A. D.; Kudrin, K. N.; Strain, M. C.; Farkas, O.; Tomasi, J.; Barone, V.; Cossi, M.; Cammi, R.; Mennucci, B.; Pomelli, C.; Adamo, C.; Clifford, S.; Ochterski, J.; Petersson, G. A.; Ayala, P. Y.; Cui, Q.; Morokuma, K.; Malick, D. K.; Rabuck, A. D.; Raghavachari, K.; Foresman, J. B.; Cioslowski, J.; Ortiz, J. V.; Baboul, A. G.; Stefanov, B. B.; Liu, G.; Liashenko, A.; Piskorz, P.; Komaromi, I.; Gomperts, R.; Martin, R. L.; Fox, D. J.; Keith, T.; Al-Laham, M. A.; Peng, C. Y.; Nanayakkara, A.; Gonzalez, C.; Challacombe, M.; Gill, P. M. W.; Johnson, B.; Chen, W.; Wong, M. W.; Andres, J. L.; Gonzalez, C.; Head-Gordon, M.; Replogle, E. S.; Pople, J. A. *GAUSSIAN 98*; Gaussian, Inc., Pittsburgh, PA, 1998.
- (53) Gonzalez, C.; Schlegel, H. B. *J. Chem. Phys.* **1989**, *90*, 2154–2161. (b) *J. Phys. Chem.* **1990**, *94*, 5523–5527.

- (54) Kwok, W. M.; Ma, C.; Parker, A. W.; Phillips, D.; Towrie, M.; Matousek, P.; Phillips, D. L. *J. Phys. Chem. A* **2003**, *107*, 2624–2628.
- (55) Kwok, W. M.; Zhao, C.; Guan, X.; Li, Y. L.; Du, Y.; Phillips, D. L. *J. Chem. Phys.* **2004**, *120*, 9017–9032.
- (56) Zheng, X.; Phillips, D. L. *J. Phys. Chem. A* **2000**, *104*, 6880–6886.
- (57) Kwok, W. M.; Ma, C.; Parker, A. W.; Phillips, D.; Towrie, M.; Matousek, P.; Phillips, D. L. *J. Chem. Phys.* **2000**, *113*, 7471–7478.
- (58) Tarnovsky, A. N.; Sundstrom, V.; Akesson, E.; Pascher, T. *J. Phys. Chem. A* **2004**, *108*, 237–249.
- (59) Kawasaki, M.; Lee, S. J.; Bersohn, R. *J. Chem. Phys.* **1975**, *63*, 809–814.
- (60) Schmitt, G.; Comes, F. J. *J. Photochem.* **1980**, *14*, 107–123.
- (61) Kroger, P. M.; Demou, P. C.; Riley, S. J. *J. Chem. Phys.* **1976**, *65*, 1823–1834.
- (62) Baughcum, S. L.; Leone, S. R. *J. Chem. Phys.* **1980**, *72*, 6531–6545.
- (63) Schwartz, B. J.; King, J. C.; Zhang, J. Z.; Harris, C. B. *Chem. Phys. Lett.* **1993**, *203*, 503–508.
- (64) Saitow, K.; Naitoh, Y.; Tominaga, K.; Yoshihara, Y. *Chem. Phys. Lett.* **1996**, *262*, 621–626.
- (65) Tarnovsky, A. N.; Alvarez, J.-L.; Yartsev, A. P.; Sundstrom, V.; Akesson, E. *Chem. Phys. Lett.* **1999**, *312*, 121–130.
- (66) Odelius, M.; Kadi, M.; Davidsson, J.; Tarnovsky, A. N. *J. Chem. Phys.* **2004**, *121*, 2208–2214.